Geophysical Research Letters®

Key Points:

- Be-10 exposure ages from moraines in the Chersky Range show that glaciers in central NE Siberia contracted over the last two glacial cycles
- Northeast Siberia hosted mountain-centered icefields during the Late Pleistocene, but no large-scale continental ice masses
- Largest ice extent in the Chersky Range predates the penultimate glacial cycle and likely occurred during the Mid-Pleistocene super-glacials

Correspondence to:

J. Nørgaard,
jn@geo.au.dk

Absence of Large-Scale Ice Masses in Central Northeast Siberia During the Late Pleistocene

Jesper Nørgaard[1], Martin Margold[2], John D. Jansen[3], Redzhep Kurbanov[4], Izabela Szuman[2,5], Jane Lund Andersen[1,6], Jesper Olsen[7], and Mads Faurschou Knudsen[1]

[1]Department of Geoscience, Aarhus University, Aarhus, Denmark, [2]Department of Physical Geography and Geoecology, Charles University, Prague, Czechia, [3]GFÚ Institute of Geophysics, Czech Academy of Sciences, Prague, Czechia, [4]Institute of Water Problems, Hydropower and Ecology, National Academy of Sciences of Tajikistan, Dushanbe, Tajikistan, [5]Institute of Geoinformation and Geoecology, Adam Mickiewicz University, Poznań, Poland, [6]Department of Physical Geography, Stockholm University, Stockholm, Sweden, [7]Department of Physics and Astronomy, Aarhus University, Aarhus, Denmark

Abstract Ongoing speculation regarding the existence of large Late Pleistocene ice masses in Northeast Eurasia reflects the dearth of age constraints on glaciations across this vast region. Here, we report the first dates from the central part of Northeast Siberia, consisting of 22 cosmogenic ^{10}Be exposure ages from boulders deriving from a sequence of three moraines in the Chersky Range. The dated moraine sequence indicates progressive contraction of maximum glacier extent from Marine Isotope Stage 6 to the Last Glacial Maximum, while the remotely-sensed mapping indicates an older, more expansive glaciation in the region yet undated. Our results show that Late Pleistocene glaciations were limited to the highlands, and Northeast Siberia did not host a large, coalescent ice sheet during the Last Glacial Maximum or Marine Isotope Stage 6.

Plain Language Summary Very little is known about the glacial history of Northeast Siberia, which has led to speculations concerning the size and timing of past ice masses in this vast region. Some have previously suggested the area was covered by a large ice sheet during the Last Glacial Maximum 20 Kyr ago, but the consensus today maintains that the ice cover was limited due to restricted moisture sources. It is clear, however, that Northeast Siberia at one point in time hosted large ice masses, as the region is home to extensive glacial landforms of unknown age. We use cosmogenic ^{10}Be exposure dating to study a glacial moraine complex with three well-defined moraine ridges in the Chersky Range located in central Northeast Siberia. Our results show that the youngest and innermost moraine was emplaced toward the end of the Last Glacial Maximum, whereas the oldest and outermost moraine was emplaced during the penultimate glaciation ~130 Kyr ago. This suggests that Northeast Siberia did not host a large ice sheet during the Late Pleistocene, and that the ice cover was limited to mountain glaciers. Satellite-based mapping of glacial landforms confirms the existence of at least one older, more expansive glaciation that remains undated.

1. Introduction

Waxing and waning ice sheets and mountain glaciers have been a defining feature of the climate oscillations during the Pleistocene ice ages. Ice masses have shaped extensive tracts of Earth's surface, modified oceanic and atmospheric circulation (Toucanne et al., 2015), and stored large volumes of water periodically, driving variations in eustatic sea level (Lambeck et al., 2014; Simms et al., 2019). Significant research efforts have been directed to constraining the Pleistocene extents and chronology of the major existing and ephemeral ice sheets (Batchelor et al., 2019) together with some of the smaller ice sheets and mountain ice masses (e.g., Ivy-Ochs et al. (2008); Licciardi and Pierce (2018)). However, substantial gaps in our knowledge persist regarding the cryosphere and its history. Most notably, we are still unable to match eustatic sea level with reconstructed ice volumes during the Last Glacial Maximum (LGM, Simms et al. (2019)), let alone for older glacial cycles. One region in need of attention is Northeast Siberia, east of the Lena River (Figure 1), where the prevailing view is that the western Eurasian Ice Sheet effectively blocked Atlantic moisture sources from reaching Siberia, promoting an extreme continental climate inimical to the growth of major ice sheets (Krinner et al., 2011; Siegert & Marsiat, 2001). And yet, the extensive mountain landscapes of this region display over one million km² of formerly glaciated terrain (Barr & Clark, 2012). Glaciation of this extent could account for several meters of global sea-level equivalent, but the timing of any such ice mass is completely unresolved. Here, we aim to provide a chronological record of past glaciation in a key area of this vast, understudied region.

Figure 1. Northeast Siberia, showing the regional setting of the study area (red box) in the Chersky Range and other locations and studies mentioned in the text. The bottom right insert shows the Northern Hemisphere maximum ice extent during the Last glacial cycle adapted from Ehlers and Gibbard (2007), Hughes et al. (2013) with the Laurentide Ice Sheet (LIS) and Eurasian Ice Sheet (EIS) marked.

The growth of ice masses in Northeast Siberia hinges upon two potential moisture sources, west and east. The westerlies provide the main source of precipitation along the western flank of the Verkhoyansk and Suntar-Khayata ranges (Figure 1). The deposits of piedmont glaciers extending west from the Verkhoyansk indicate progressively smaller ice advances through time, as shown by optically stimulated luminescence ages of 140 to 50 ka from intercalated aeolian and fluvial sediments (Stauch & Lehmkuhl, 2010; Stauch et al., 2007). To the east, at the opposite periphery, the Pacific Ocean is the predominant source of precipitation. Cosmogenic ^{36}Cl exposure ages from the Kuveveem and Tanyurer valleys (Figure 1) indicate small-scale mountain glaciation at the LGM along with evidence of at least one prior, more extensive glacial advance (Brigham-Grette et al., 2003; Gualtieri et al., 2000). While on-land evidence is lacking for a former mountain-centered ice sheet thick enough to behave independently of the underlying topography (Barr & Clark, 2012), glacial landforms discovered on the northern continental shelf suggest an ice sheet up to 1 km thick (Figure 1; Niessen et al. (2013)). Such an ice sheet may have grown repeatedly prior to the LGM, but whether it coalesced with mountain-centered ice masses remains an open question. Geomorphic evidence indicates that the extensive ice sheet on the continental shelf predates the LGM and most likely took place during Marine Isotope Stage (MIS) 6 (Jakobsson et al., 2016).

In between the Verkhoyansk Range to the west, the Pacific Ocean to the east and the Arctic Ocean to the north, there is a ~2,000 × 1,500 km expanse that includes the Suntar-Khayata Range, the Kolyma Highlands and the Chersky Range (Figure 1). This area remains something of a blank spot in terms of moisture availability and glacial history. Here, we present the first cosmogenic ^{10}Be exposure ages from the Chersky Range, the highest mountains in Northeast Siberia at just over 3,000 m above sea level (masl). We target a glacial moraine sequence at Lake Malyk with three well-defined ridges formed by an outlet glacier that emanated from a mountain icefield flanked by peaks up to ~2,300 masl. (Figures 2 and 3).
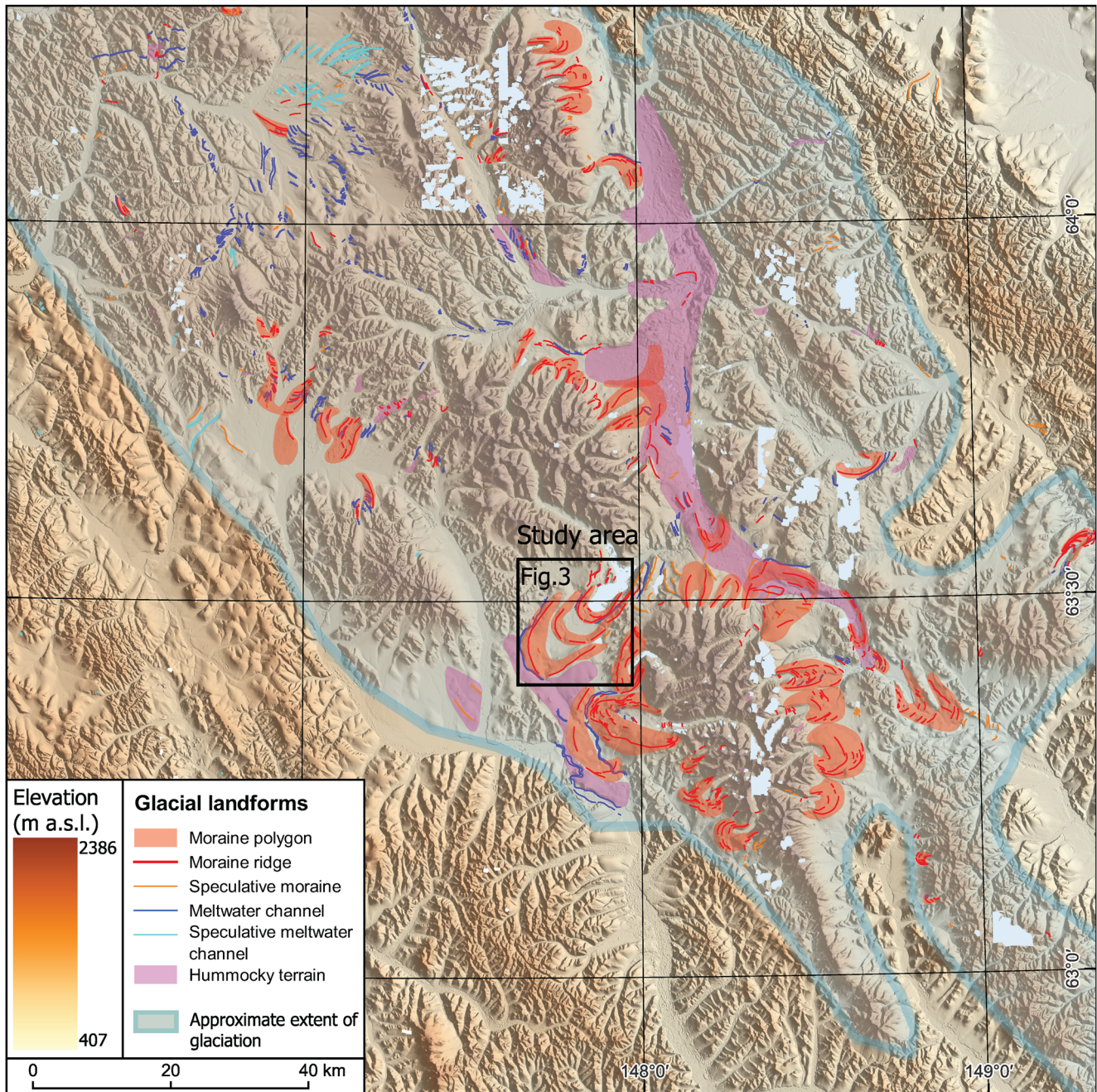
Figure 2. Geomorphological mapping of the area surrounding the study site. The overview indicates that the dated moraines are not representative of the largest glaciations in the Chersky Range. The maximum extent of glaciation (light blue outline) remains undated.

2. Methods

The three moraine ridges at Lake Malyk were identified in the regional moraine inventory of Barr and Clark (2012). We mapped the surrounding mountain topography from the high-resolution digital elevation model ArcticDEM (Morin et al. (2016), http://arcticDEM.org) to gain a complete glacial geomorphological overview of the study area (Figure 2).

Fieldwork was carried out in late summer 2021. The moraine ridges were accessed on foot, while searching for suitable ice-transported boulders to sample for cosmogenic [10]Be exposure dating. Boulders were few and scattered sparsely across the moraines, hence all those that we deemed of suitable size and in good condition were sampled
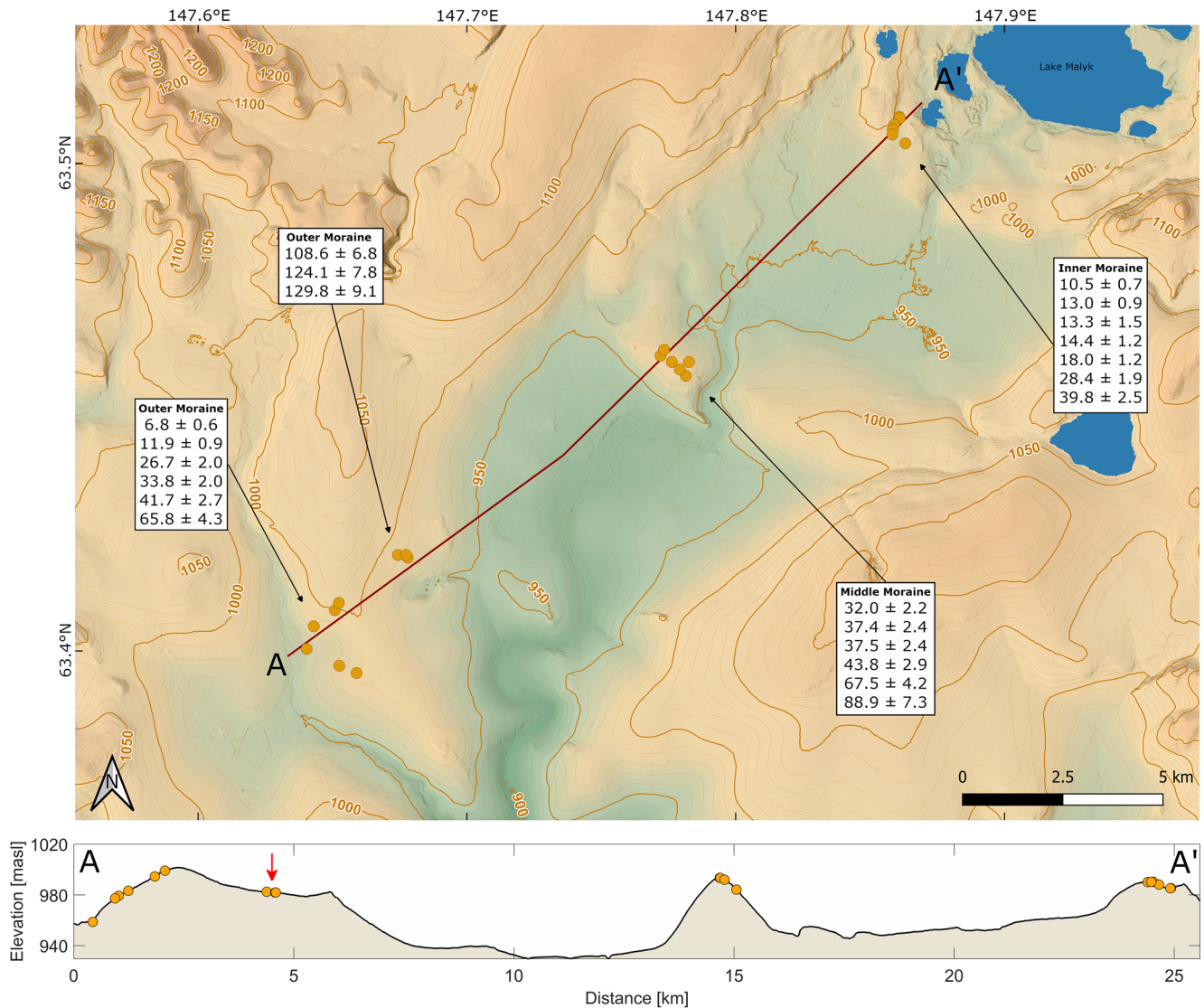
Figure 3. Top panel shows the Lake Malyk valley, including the three transverse end-moraines and sampling locations (orange dots). Boxes show the exposure ages within the sample clusters. The lower panel shows a topographic profile through the transect in the upper panel (A-A'), highlighting the differing moraine morphologies (sample elevations are projected onto the profile). The red arrow on the outer moraine points to the key samples MS-M1,5B-1, MS-M1,5B-2, and MS-M1,5B-3 in a position less vulnerable to post-depositional instability.

with an electric angle-grinder targeting the uppermost 2–3 cm. A total of 22 moraine boulders were sampled and analyzed; 9 samples from the outer moraine ridge, 6 from the middle moraine, and 7 from the inner moraine (Table 1, Figure 3). All sampled boulders were of granitic composition and none showed evidence of surface spalling suggestive of frost action despite the extremely low winter temperatures characteristic for the region.

To determine the abundance of cosmogenic ^{10}Be in the boulder samples, and thereby constrain their depositional age, we employed the Aarhus University cosmogenic nuclides laboratory and accelerator mass spectrometry center (see Supporting Information S1 for full details on procedures and AMS results). Exposure ages were derived from the online calculators formerly known as the CRONUS-Earth online calculators, version 3 (Balco et al., 2008), using the time-dependent scaling scheme (LSDn) of Lifton et al. (2014) (Table 1).

3. Results

Our mapping reveals an area of hummocky terrain in the forefield of the Lake Malyk moraine sequence, displacing the course of the Berelyokh River to the foot of the lower mountains in the west (see Figure 2). We interpret

Table 1
Summary of Cosmogenic Nuclide Data

Sample ID	Lat	Long	Elevation (m a.s.l.)	^{10}Be conc. (10^5 at/g)	^{10}Be uncert. (10^5 at/g)	Sample thickness (cm)	Boulder height (cm)	LSDn age (ka)	LSDn 1-σ exter. Error (ka)
Outer Moraine									
MS-MB-4	63.425	147.668	991	0.763	0.051	3	30	6.8	0.6
MS-MB-2	63.423	147.662	965	1.312	0.069	3	50	11.9	0.9
MS-MB-1	63.420	147.660	950	2.901	0.132	2.5	65	26.7	2.0
MS-MB-10	63.418	147.669	967	3.741	0.031	2	15	33.8	2.0
MS-MB-5	63.426	147.669	993	4.669	0.110	3	40	41.7	2.7
MS-MB-12	63.417	147.674	980	7.274	0.193	2.5	55	65.8	4.3
MS-M1,5B-2	63.432	147.685	984	11.873	0.170	3	130	108.6	6.8
MS-M1,5B-1	63.431	147.688	982	13.717	0.202	1	130	124.1	7.8
MS-M1,5B-3	63.432	147.687	980	14.243	0.475	1.5	150	129.8	9.1
Middle Moraine									
MS-M2B-2	63.456	147.765	998	3.605	0.126	3	65	32.0	2.2
MS-M2B-6	63.456	147.760	988	4.208	0.112	2	65	37.4	2.4
MS-M2B-3	63.454	147.764	987	4.203	0.085	2.5	55	37.5	2.4
MS-M2B-4	63.455	147.763	983	4.899	0.128	2	60	43.8	2.9
MS-M2B-7	63.456	147.757	987	7.539	0.110	2	100	67.5	4.2
MS-M2B-8	63.457	147.758	985	9.894	0.543	1.5	60	88.9	7.3
Inner Moraine									
MS-M3B-9	63.484	147.821	972	1.174	0.041	1.5	25	10.5	0.7
MS-M3B-8	63.484	147.821	978	1.455	0.044	2	35	13.0	0.9
MS-M3B-4	63.485	147.822	986	1.504	0.147	2	60	13.3	1.5
MS-M3B-1	63.486	147.823	975	1.592	0.094	3	80	14.4	1.2
MS-M3B-3	63.486	147.823	974	2.012	0.062	2	60	18.0	1.2
MS-M3B-11	63.482	147.825	966	3.138	0.085	2	200	28.4	1.9
MS-M3B-7	63.484	147.821	978	4.442	0.081	2	80	39.8	2.5

Note. Geographical coordinates and elevation above sea level were measured with a handheld GPS. Sample thickness and boulder height were estimated in the field with a tape measure. Ages reported are calculated with the online calculator formerly known as the CRONUS-Earth online calculators, version 3 (Balco et al., 2008) with an assumed rock density 2.65 g cm^{-3}, a boulder erosion of 0 m yr^{-1} and the time-dependent scaling scheme (LSDn) of Lifton et al. (2014). All ages are corrected for topographic shielding (additional details in Table S1 in Supporting Information S1).

this area as a degraded moraine from a glaciation that extended well beyond the Lake Malyk moraines. This is in line with the maximum extent of the mountain ice field, identified from the mapped glacial geomorphological record elsewhere around its periphery (Figure 2).

Of the three sampled moraines, the outermost moraine ridge of the Lake Malyk sequence is the largest and seemingly most denuded given its flattish slopes. The samples from the outer moraine were mainly collected from the distal slope and moraine crest (Figure 3), but three samples were also collected from the gentler dipping proximal side of the moraine (red arrow in Figure 3). The middle and inner moraines are of similar size and degree of degradation, and on both moraines, samples were collected close to the crest. The three moraines are sparsely covered by open-canopy mountain taiga with undergrowth of shrubs, lichen and mosses; the only moraine materials exposed are boulders and blocks ranging from a few tens of centimeters to several meters in diameter.

Apparent exposure ages of the nine outer moraine boulders (Figure 3) range widely between ~7 and 130 ka, including an age cluster consisting of the three individual ages 109 ± 7, 124 ± 8, and 130 ± 9 ka associated with the three large blocks on the moraine's proximal side. The six boulders of the middle moraine yielded ages
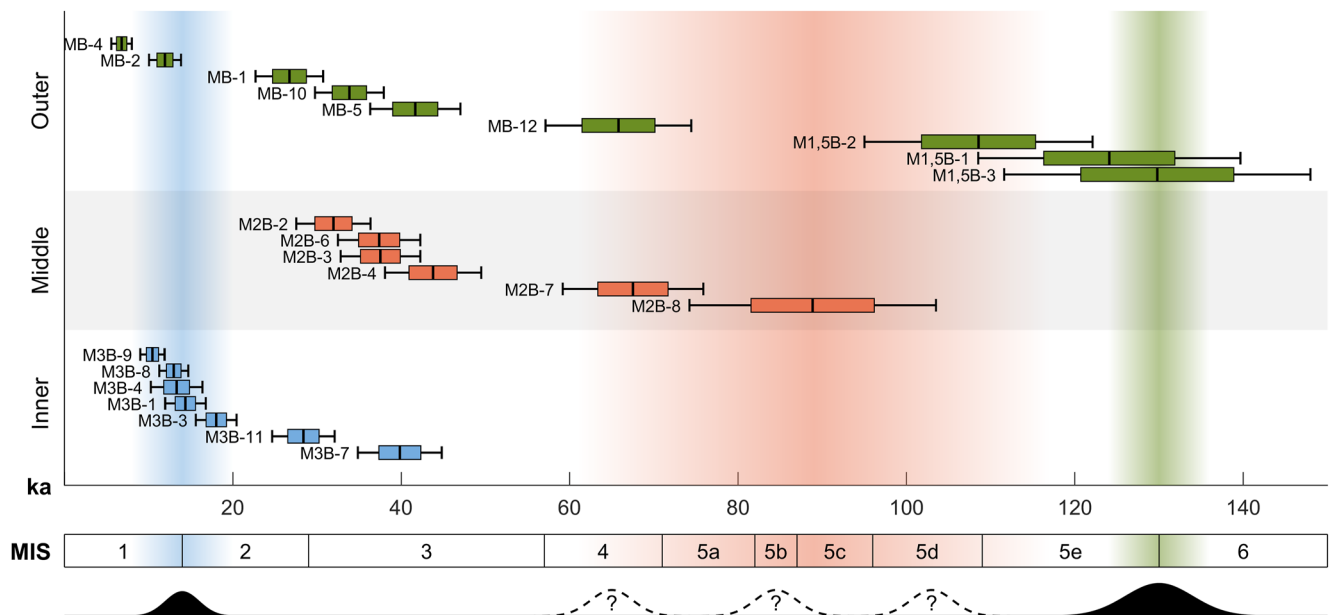
Figure 4. Boulder exposure ages for the outer, middle and inner moraines shown with 1-σ (box) and 2-σ (whisker) uncertainties. Fading colors in the background indicate interpreted moraine ages (green = outer moraine, orange = middle, blue = inner). The lowermost panel is a visualization of the inferred age of the glaciations at Lake Malyk.

between 32.0 ± 2.2 and 88.9 ± 7.3 ka, and the seven inner moraine boulders yielded ages between 10.5 ± 0.7 and 39.8 ± 2.5 ka (Table 1).

Corrections for cosmic-ray shielding owing to topography, vegetation, and snow cover, were calculated according to Gosse and Phillips (2001). Topographic shielding estimated from field observations is included in our age calculations (Table 1). Shielding by vegetation was deemed negligible due to the sparse plant cover (Figure S1 in Supporting Information S1). Snow shielding was estimated from the nearest meteorological stations in Yakutsk and Magadan; these suggest a 50 cm snow cover for 8 months per year, but given the stations are located in the lowlands and far from our field site, we acknowledge the high uncertainty of these estimates. As a safeguard, we calculate the snow shielding estimate for both 50 and 100 cm snow cover for 8 months per year, which effectively increases our exposure ages by ~4% and ~8%, respectively. Such effects exert little influence on our study findings, so instead we suffice by providing the complete shielding corrections in Table S1 in Supporting Information S1.

4. Discussion

4.1. Boulder Exposure Ages at Lake Malyk

Two geological sources contribute to the often-observed scatter in boulder exposure ages in moraines: (a) post-depositional shielding linked to the movement of boulders on the moraine or their exhumation over time; and (b) pre-depositional exposure, the persistence of nuclides inherited from exposure prior to moraine deposition (Applegate et al., 2010; Fabel & Harbor, 1999; Heyman et al., 2011). Post-depositional shielding yields exposure ages that underestimate moraine age, whereas inheritance gives rise to ages that are too old. Such factors are important to consider at Lake Malyk given that the exposure ages scatter so widely that the moraine ages all apparently overlap (Figure 4). And yet, the three moraine ridges are assumed a priori to be progressively older from inner to outer, as we expect the glacier to remove or at least smooth any existing ridges that it overwrites on re-advancement. How to address this issue?

First, all moraine ridges are subject to gradual surface lowering and reshaping via diffusional processes, especially those like at Lake Malyk that can, due to the climate of the region, be assumed to be partially ice-cored. The degree of reshaping can be expected to increase with time, thereby enhancing post-depositional shielding effects on boulders in the moraine and skewing the exposure age distribution toward too-young ages (Heyman

et al., 2011; Putkonen & Swanson, 2003). We can recognize this effect in the notable increase in age scatter from the inner, younger ridge to the outer, older and more intensely denuded ridge (ranging ∼ 29 and 123 Kyr, respectively) (Figure 4). Second, nuclide inheritance is also a common feature. For instance, it is identified in 27% (n = 590) of ice-transported, exposure dated boulders in Fennoscandia (Jansen et al., 2019). While nuclide inheritance in moraine boulders is largely stochastic, it exerts a disproportionate effect on younger moraines because any inheritance present will comprise a larger fraction of the apparent age.

The notion that age scatter at the outer moraine is the result of post-depositional shielding is consistent with the positive relationship we observe between exposure age and boulder height above ground on the outer ridge (Table 1, Figure S2 in Supporting Information S1, Heyman et al. (2016)). That same trend is also present (albeit weaker) at the middle moraine but it is largely absent at the inner moraine, reflecting the difference in post-depositional modifications between moraines. Accordingly, we hinge our interpretation of the outer moraine age on the three oldest, well clustered samples (MS-M1,5B-1, MS-M1,5B-2, MS-M1,5B-3), which indicate deposition toward the end of MIS 6 (Figure 4). The apparent stability of these three boulders sets them apart in our data set. They all stand >130 cm above ground-level, which is more than two-fold taller than the other outer moraine boulders (Table 1), and they rest on the flattish proximal side of the moraine (Figure 3), which presumably protected them from any post-depositional slope activity.

For the middle moraine, we also invoke post-depositional shielding as the main driver of the age scatter (∼89–32 ka); hence, we interpret the oldest ages to be most representative of the moraine age (Applegate et al., 2012; Putkonen & Swanson, 2003). The oldest sample, M2B-8, spans MIS 4 and both glacial sub-stages of MIS 5 (Figure 4) making it hard to distinguish between these. Nevertheless, in accordance with our a priori model of the relative ages, the middle moraine likely arose during one of these periods, but we cannot rule out that it arose during MIS 3.

The seven boulder ages of the inner moraine are generally younger and closer in agreement with each other than for the outer and middle moraines. Following our model noted above, here we consider that the age scatter derives mainly from nuclide inheritance via pre-depositional exposure. We envisage the likely scenario in which boulders transported by the earlier ice advances are incorporated into the inner moraine. This would result in some of the boulder exposure ages being older than the moraine itself (Heyman et al., 2011); namely samples MS-M3B-7 and MS-M3B-11. The remaining ages place the deposition of the inner moraine to after stabilization at the end of the global LGM.

4.2. Siberian and Northern Hemisphere Glacial Contraction Since Middle Pleistocene

Our results represent the first robust glacial chronology for the central portion of Northeast Siberia that extends beyond MIS 2. Combined with previous findings from peripheral areas, we identify a regional pattern of glaciation despite the putative diversity of moisture sources. LGM glacier extents fall inside those recorded during earlier stadials of the last glacial cycle (Brigham-Grette et al., 2003; Stauch & Lehmkuhl, 2010; Stauch et al., 2007), which are in turn less than glacier extents dated to the penultimate glacial maximum (the MIS 6 peak at ∼150–135 ka (Stauch & Lehmkuhl, 2010; Stauch et al., 2007)). Furthermore, based on our geomorphological mapping of the Chersky Range, we suggest that even greater glacial extents preceded the MIS 6 glaciation (Figure 2), but these remain undated.

An emergent picture of contracting ice extents, both for ice sheet and mountain glaciation, during the Middle and Late Pleistocene is shared by other regions with continental climates extending geographically over both Eurasia and North America. It applies to the eastern margin of the Eurasian Ice Sheet (Astakhov et al., 2016; Svendsen et al., 2004), the Cordilleran Ice Sheet margin in the Yukon (Hidy et al., 2013; Ward et al., 2017), as well as to the mountain ice masses of Alaska (Briner & Kaufman, 2008; Kaufman & Manley, 2004), northern High Asia (Blomdin et al., 2016) and southern-central Siberia (Margold et al., 2016). Like others before us (Barr & Clark, 2011; Stauch & Gualtieri, 2008; Stauch et al., 2007), we speculate that these contracting continental ice masses reflect the moisture-starved conditions caused by the massive bulk of the Laurentide and Eurasian ice sheets, which effectively divert atmospheric circulation patterns during glacial maxima (Krinner et al., 2011; Löfverström et al., 2014; Yanase & Abe-Ouchi, 2010). However, we cannot completely exclude the possibility that the climatic conditions at Lake Malyk stayed relatively constant during periods of glacier build-up, and that the erosional feedback and geomorphological changes from previous advancements were responsible for the shortening of the glacier (Anderson et al., 2012; Rowan et al., 2022).

In most of the continental regions noted above, the timing of Pleistocene glacial maxima remains unresolved or problematic. Considering the reconstructed ice extents relative to the global ice volumes implied by the $\delta^{18}O$ record (Lisiecki & Raymo, 2005), we confirm that continental Northeast Siberia did not host the "missing LGM ice sheet" (Simms et al., 2019). Indeed, if a large ice sheet did develop somewhere in Northeast Siberia during the LGM, it seems unlikely that it coincided with minimal ice extent in the western periphery (the Verkhoyansk Range, Stauch and Lehmkuhl (2010)), the eastern periphery (the Pacific Ocean, (Brigham-Grette et al., 2003; Gualtieri et al., 2000)), and the central part of Northeast Siberia (the Chersky Range (this study)). Additionally, proxy-based temperature reconstructions indicate that the temperature decrease was minimal in Northeast Siberia and Beringia during the LGM (Osman et al., 2021). Given the reasonably limited ice extent in the Chersky Range and the Verkhoyansk Range toward the end of MIS 6, some ∼130 Kyr ago, a large ice sheet connecting the various mountain icefields in the Northeast Siberia also seems unlikely during the penultimate glacial period. With regard to the yet unconstrained Pleistocene maximum glacier advance in this region, we favor one of the super-glacials of the Middle Pleistocene (MIS 16 or 12), or the more recent MIS 10. An Early Pleistocene maximum is also plausible, given the first major advance of the Cordilleran Ice Sheet at ∼ 2.8–2.4 Ma (Hidy et al., 2013). However, this would exacerbate the difficulty of matching the low global ice volumes of the Early Pleistocene (Lisiecki & Raymo, 2005) with regionally extensive ice masses (Balco & Rovey, 2010; Hidy et al., 2013).

5. Conclusion

We have presented 22 new cosmogenic ^{10}Be exposure ages from glacially-transported boulders in the Chersky Range, the highest mountains of Northeast Siberia, where the glacial history was so far undated. The ages from our three distinct end-moraines are strongly influenced by geological processes, causing partial cosmic-ray shielding and/or inheritance of nuclides. Taking into account these complications, the tripartite-moraine system is interpreted to comprise a MIS 6 outer moraine, a LGM inner moraine, and an intermediate moraine that likely was deposited during MIS 4 or 5. Our findings reveal a progressively smaller glacier footprint in Northeast Siberia since MIS 6. The shrinking trend likely reflects the effects of extreme continentality and/or the development of moisture-blocking ice masses in western Eurasia and North America. Akin to studies reporting from the periphery of Northeast Siberia (Brigham-Grette et al., 2003; Gualtieri et al., 2000; Stauch & Lehmkuhl, 2010; Stauch et al., 2007), we show that Late Pleistocene glaciations in the Chersky Range were limited to alpine-type valley glaciers. A large coalescent ice sheet, or "missing LGM ice sheet" (Simms et al., 2019) did not develop here during the Late Pleistocene. We mapped traces of the local Pleistocene maximum glacial extent that we tentatively link to one of the super-glacials MIS 16 or 12, or the more recent MIS 10. However, the question of whether the mountain-centered ice masses coalesced into a larger ice sheet conjoined with the glaciation on the continental shelf (cf. Niessen et al., 2013) requires further investigation.

Data Availability Statement

All data used for the publication can be accessed via the link: https://doi.org/10.5281/zenodo.7715017.

References

Anderson, R. S., Dühnforth, M., Colgan, W., & Anderson, L. (2012). Far-flung moraines: Exploring the feedback of glacial erosion on the evolution of glacier length. *Geomorphology*, *179*, 269–285. https://doi.org/10.1016/j.geomorph.2012.08.018

Applegate, P. J., Urban, N. M., Keller, K., Lowell, T. V., Laabs, B. J. C., Kelly, M. A., & Alley, R. B. (2012). Improved moraine age interpretations through explicit matching of geomorphic process models to cosmogenic nuclide measurements from single landforms. *Quaternary Research*, *77*(2), 293–304. https://doi.org/10.1016/j.yqres.2011.12.002

Applegate, P. J., Urban, N. M., Laabs, B. J. C., Keller, K., & Alley, R. B. (2010). Modeling the statistical distributions of cosmogenic exposure dates from moraines. *Geoscientific Model Development*, *3*(1), 293–307. https://doi.org/10.5194/gmd-3-293-2010

Astakhov, V., Shkatova, V., Zastrozhnov, A., & Chuyko, M. (2016). Glaciomorphological map of the Russian Federation. *Quaternary International*, *420*, 4–14. https://doi.org/10.1016/j.quaint.2015.09.024

Balco, G., & Rovey, C. W. (2010). Absolute chronology for major Pleistocene advances of the Laurentide Ice Sheet. *Geology*, *38*(9), 795–798. https://doi.org/10.1130/g30946.1

Balco, G., Stone, J. O., Lifton, N. A., & Dunai, T. J. (2008). A complete and easily accessible means of calculating surface exposure ages or erosion rates from 10Be and 26Al measurements. *Quaternary Geochronology*, *3*(3), 174–195. https://doi.org/10.1016/j.quageo.2007.12.001

Barr, I. D., & Clark, C. D. (2011). Glaciers and climate in Pacific Far NE Russia during the Last Glacial Maximum. *Journal of Quaternary Science*, *26*(2), 227–237. https://doi.org/10.1002/jqs.1450

Barr, I. D., & Clark, C. D. (2012). Late Quaternary glaciations in Far NE Russia; combining moraines, topography and chronology to assess regional and global glaciation synchrony. *Quaternary Science Reviews*, *53*, 72–87. https://doi.org/10.1016/j.quascirev.2012.08.004

Batchelor, C. L., Margold, M., Krapp, M., Murton, D. K., Dalton, A. S., Gibbard, P. L., et al. (2019). The configuration of Northern Hemisphere ice sheets through the Quaternary. *Nature Communications*, *10*(1), 3713. https://doi.org/10.1038/s41467-019-11601-2

Blomdin, R., Heyman, J., Stroeven, A. P., Hättestrand, C., Harbor, J. M., Gribenski, N., et al. (2016). Glacial geomorphology of the Altai and Western Sayan Mountains, Central Asia. *Journal of Maps*, *12*(1), 123–136. https://doi.org/10.1080/17445647.2014.992177

Brigham-Grette, J., Gualtieri, L. M., Glushkova, O. Y., Hamilton, T. D., Mostoller, D., & Kotov, A. (2003). Chlorine-36 and C-14 chronology support a limited last glacial maximum across central Chukotka, northeastern Siberia, and no Beringian ice sheet. *Quaternary Research*, *59*(3), 386–398. https://doi.org/10.1016/s0033-5894(03)00058-9

Briner, J. P., & Kaufman, D. S. (2008). Late Pleistocene mountain glaciation in Alaska: Key chronologies. *Journal of Quaternary Science*, *23*(6–7), 659–670. https://doi.org/10.1002/jqs.1196

Ehlers, J., & Gibbard, P. L. (2007). The extent and chronology of Cenozoic global glaciation. *Quaternary International*, *164–165*, 6–20. https://doi.org/10.1016/j.quaint.2006.10.008

Fabel, D., & Harbor, J. (1999). The use of in-situ produced cosmogenic radionuclides in glaciology and glacial geomorphology. *Annals of Glaciology*, *28*, 103–110. https://doi.org/10.3189/172756499781821968

Gosse, J. C., & Phillips, F. M. (2001). Terrestrial in situ cosmogenic nuclides: Theory and application. *Quaternary Science Reviews*, *20*(14), 1475–1560. https://doi.org/10.1016/s0277-3791(00)00171-2

Gualtieri, L., Glushkova, O. Y., & Brigham-Grette, J. (2000). Evidence for restricted ice extent during the last glacial maximum in the Koryak Mountains of Chukotka, far eastern Russia. *GSA Bulletin*, *112*(7), 1106–1118. https://doi.org/10.1130/0016-7606(2000)112<1106:efried>2.0.co;2

Heyman, J., Applegate, P. J., Blomdin, R., Gribenski, N., Harbor, J. M., & Stroeven, A. P. (2016). Boulder height – Exposure age relationships from a global glacial 10Be compilation. *Quaternary Geochronology*, *34*, 1–11. https://doi.org/10.1016/j.quageo.2016.03.002

Heyman, J., Stroeven, A. P., Harbor, J. M., & Caffee, M. W. (2011). Too young or too old: Evaluating cosmogenic exposure dating based on analysis of compiled boulder exposure ages. *Earth and Planetary Science Letters*, *302*(1–2), 71–80. https://doi.org/10.1016/j.epsl.2010.11.040

Hidy, A. J., Gosse, J. C., Froese, D. G., Bond, J. D., & Rood, D. H. (2013). A latest Pliocene age for the earliest and most extensive Cordilleran Ice Sheet in northwestern Canada. *Quaternary Science Reviews*, *61*, 77–84. https://doi.org/10.1016/j.quascirev.2012.11.009

Hughes, P. D., Gibbard, P. L., & Ehlers, J. (2013). Timing of glaciation during the last glacial cycle: Evaluating the concept of a global 'Last Glacial Maximum' (LGM). *Earth-Science Reviews*, *125*, 171–198. https://doi.org/10.1016/j.earscirev.2013.07.003

Ivy-Ochs, S., Kerschner, H., Reuther, A., Preusser, F., Heine, K., Maisch, M., et al. (2008). Chronology of the last glacial cycle in the European Alps. *Journal of Quaternary Science*, *23*(6–7), 559–573. https://doi.org/10.1002/jqs.1202

Jakobsson, M., Nilsson, J., Anderson, L., Backman, J., Bjork, G., Cronin, T. M., et al. (2016). Evidence for an ice shelf covering the central Arctic Ocean during the penultimate glaciation. *Nature Communications*, *7*(1), 10365. https://doi.org/10.1038/ncomms10365

Jansen, J. D., Knudsen, M. F., Andersen, J. L., Heyman, J., & Egholm, D. L. (2019). Erosion rates in Fennoscandia during the past million years. *Quaternary Science Reviews*, *207*, 37–48. https://doi.org/10.1016/j.quascirev.2019.01.010

Kaufman, D. S., & Manley, W. F. (2004). Pleistocene Maximum and Late Wisconsinan glacier extents across Alaska, U.S.A. *Developments in Quaternary Science*, *2*, 9–27.

Krinner, G., Diekmann, B., Colleoni, F., & Stauch, G. (2011). Global, regional and local scale factors determining glaciation extent in Eastern Siberia over the last 140,000 years. *Quaternary Science Reviews*, *30*(7–8), 821–831. https://doi.org/10.1016/j.quascirev.2011.01.001

Lambeck, K., Rouby, H., Purcell, A., Sun, Y., & Sambridge, M. (2014). Sea level and global ice volumes from the Last Glacial Maximum to the Holocene. *Proceedings of the National Academy of Sciences of the United States of America*, *111*(43), 15296–15303. https://doi.org/10.1073/pnas.1411762111

Licciardi, J. M., & Pierce, K. L. (2018). History and dynamics of the Greater Yellowstone Glacial System during the last two glaciations. *Quaternary Science Reviews*, *200*, 1–33. https://doi.org/10.1016/j.quascirev.2018.08.027

Lifton, N., Sato, T., & Dunai, T. J. (2014). Scaling in situ cosmogenic nuclide production rates using analytical approximations to atmospheric cosmic-ray fluxes. *Earth and Planetary Science Letters*, *386*, 149–160. https://doi.org/10.1016/j.epsl.2013.10.052

Lisiecki, L. E., & Raymo, M. E. (2005). A Pliocene-Pleistocene stack of 57 globally distributed benthic δ^{18}O records. *Paleoceanography*, *20*(1), PA1003. https://doi.org/10.1029/2004pa001071

Löfverström, M., Caballero, R., Nilsson, J., & Kleman, J. (2014). Evolution of the large-scale atmospheric circulation in response to changing ice sheets over the last glacial cycle. *Climate of the Past*, *10*(4), 1453–1471. https://doi.org/10.5194/cp-10-1453-2014

Margold, M., Jansen, J. D., Gurinov, A. L., Codilean, A. T., Fink, D., Preusser, F., et al. (2016). Extensive glaciation in Transbaikalia, Siberia, at the Last Glacial Maximum. *Quaternary Science Reviews*, *132*, 161–174. https://doi.org/10.1016/j.quascirev.2015.11.018

Morin, P., Porter, C., Cloutier, M., Howat, I., Noh, M. J., Willis, M., & al, e. (2016). ArcticDEM; a publically available, high resolution elevation model of the Arctic EGu General Assembly Conference Abstracts (Vol. *18*). 8396.

Niessen, F., Hong, J. K., Hegewald, A., Matthiessen, J., Stein, R., Kim, H., et al. (2013). Repeated Pleistocene glaciation of the East Siberian continental margin. *Nature Geoscience*, *6*(10), 842–846. https://doi.org/10.1038/ngeo1904

Osman, M. B., Tierney, J. E., Zhu, J., Tardif, R., Hakim, G. J., King, J., & Poulsen, C. J. (2021). Globally resolved surface temperatures since the Last Glacial Maximum. *Nature*, *599*(7884), 239–244. https://doi.org/10.1038/s41586-021-03984-4

Putkonen, J., & Swanson, T. (2003). Accuracy of cosmogenic ages for moraines. *Quaternary Research*, *59*(2), 255–261. https://doi.org/10.1016/s0033-5894(03)00006-1

Rowan, A. V., Egholm, D. L., & Clark, C. D. (2022). Forward modelling of the completeness and preservation of palaeoclimate signals recorded by ice-marginal moraines. *Earth Surface Processes and Landforms*, *47*(9), 2198–2208. https://doi.org/10.1002/esp.5371

Siegert, M. J., & Marsiat, I. (2001). Numerical reconstructions of LGM climate across Eurasian Arctic. *Quaternary Science Reviews*, *20*(15), 1595–1605. https://doi.org/10.1016/s0277-3791(01)00017-8

Simms, A. R., Lisiecki, L., Gebbie, G., Whitehouse, P. L., & Clark, J. F. (2019). Balancing the last glacial maximum (LGM) sea-level budget. *Quaternary Science Reviews*, *205*, 143–153. https://doi.org/10.1016/j.quascirev.2018.12.018

Stauch, G., & Gualtieri, L. (2008). Late Quaternary glaciations in northeastern Russia. *Journal of Quaternary Science*, *23*(6–7), 545–558. https://doi.org/10.1002/jqs.1211

Stauch, G., & Lehmkuhl, F. (2010). Quaternary glaciations in the Verkhoyansk Mountains, Northeast Siberia. *Quaternary Research*, *74*(1), 145–155. https://doi.org/10.1016/j.yqres.2010.04.003

Stauch, G., Lehmkuhl, F., & Frechen, M. (2007). Luminescence chronology from the Verkhoyansk Mountains (North-Eastern Siberia). *Quaternary Geochronology*, *2*(1–4), 255–259. https://doi.org/10.1016/j.quageo.2006.05.013

Svendsen, J. I., Alexanderson, H., Astakhov, V. I., Demidov, I., Dowdeswell, J. A., Funder, S., et al. (2004). Late Quaternary ice sheet history of northern Eurasia. *Quaternary Science Reviews*, *23*(11–13), 1229–1271. https://doi.org/10.1016/j.quascirev.2003.12.008

Toucanne, S., Soulet, G., Freslon, N., Silva Jacinto, R., Dennielou, B., Zaragosi, S., et al. (2015). Millennial-scale fluctuations of the European Ice Sheet at the end of the last glacial, and their potential impact on global climate. *Quaternary Science Reviews*, *123*, 113–133. https://doi.org/10.1016/j.quascirev.2015.06.010

Ward, B. C., Bond, J. D., & Gosse, J. C. (2017). Evidence for a 55–50 ka (early Wisconsin) glaciation of the Cordilleran ice sheet, Yukon Territory, Canada. *Quaternary Research*, *68*(1), 141–150. https://doi.org/10.1016/j.yqres.2007.04.002

Yanase, W., & Abe-Ouchi, A. (2010). A numerical study on the atmospheric circulation over the midlatitude North Pacific during the last glacial maximum. *Journal of Climate*, *23*(1), 135–151. https://doi.org/10.1175/2009jcli3148.1

References From the Supporting Information

Nishiizumi, K., Imamura, M., Caffee, M. W., Southon, J. R., Finkel, R. C., & McAninch, J. (2007). Absolute calibration of 10Be AMS standards. *Nuclear Instruments and Methods in Physics Research Section B: Beam Interactions with Materials and Atoms*, *258*(2), 403–413. https://doi.org/10.1016/j.nimb.2007.01.297